Biochimica et Biophysica Acta 1818 (2012) 64–71

Contents lists available at SciVerse ScienceDirect

Biochimica et Biophysica Acta

journal homepage: www.elsevier.com/locate/bbamem

A consensus segment in the M2 domain of the hP2X$_7$ receptor shows ion channel activity in planar lipid bilayers and in biological membranes

Cristina Alves Magalhães de Souza [a,b], Pedro Celso Nogueira Teixeira [a], Robson Xavier Faria [a], Oxana Krylova [b], Peter Pohl [c], Luiz Anastacio Alves [a,*]

[a] Oswaldo Cruz Foundation, Oswaldo Cruz Institute, Laboratory of Cellular Communication, Av. Brazil 4365, 21045-900, Rio de Janeiro, Brazil
[b] Leibniz Institute for Molecular Pharmacology, Berlin, Germany
[c] Institut für Biophysik, Johannes Kepler Universität, Altenberger Str. 69, A-4040, Linz, Austria

ARTICLE INFO

Article history:
Received 26 April 2011
Received in revised form 2 September 2011
Accepted 13 September 2011
Available online 17 September 2011

Keywords:
P2X$_7$ receptor
Ionic channel activity
Peptide single channel activity
Artificial planar lipid bilayer
Patch-clamp

ABSTRACT

The P2X$_7$ receptor (P2X$_7$R) is an ATP-gated, cation-selective channel permeable to Na^+, K^+ and Ca^{2+}. This channel has also been associated with the opening of a non-selective pore that allows the flow of large organic ions. However, the biophysical properties of the P2X$_7$R have yet to be characterized unequivocally. We investigated a region named ADSEG, which is conserved among all subtypes of P2X receptors (P2XRs). It is located in the M2 domain of hP2X$_7$R, which aligns with the H5 signature sequence of potassium channels. We investigated the channel forming ability of ADSEG in artificial planar lipid bilayers and in biological membranes using the cell-attached patch-clamp techniques. ADSEG forms channels, which exhibit a preference for cations. They are voltage independent and show long-term stability in planar lipid bilayers as well as under patch-clamping conditions. The open probability of the ADSEG was similar to that of native P2X$_7$R. The conserved part of the M2 domain of P2X$_7$R forms ionic channels in planar lipid bilayers and in biological membranes. Its electrophysiological characteristics are similar to those of the whole receptor. Conserved and hydrophobic part of the M2 domain forms ion channels.

1. Introduction

Nucleotides and nucleosides, such as ATP and adenosine, respectively, provide a wide variety of biological functions, including serving as energy carriers, forming the backbone of nucleic acids and acting as substrates for different enzymes. Moreover, they behave as extracellular messengers with important biological functions through the recognition by cellular membrane receptors, designated P1 and P2 receptors [1–3]. The P1 receptors have adenosine as their major ligand and are associated with adenylate cyclase activity. The P2Rs have ATP, UTP, ADP and UDP as their principal physiological ligands and are subdivided into the classes P2X receptors (ligand-gated ion channels) and P2Y receptors (G protein-coupled receptors) [4]. The cloning of cDNAs that encode P2R has demonstrated that there are seven P2X subtypes, denoted P2X$_{1-7}$ [5].

P2X$_7$R differ in many respects from the other subtypes of the P2X family [6]. The main distinguishing pharmacological properties of this receptor are (i) a low-agonist potency of ATP (considerably smaller than that of its structural analog dibenzoyl-ATP (BzATP)), (ii) inhibition by various divalent cations including Ca^{2+} and Mg^{2+}, and (iii) blockade of the ATP effect by a range of selective antagonists, such as pyridoxalphosphate-6-azopheryl-2′,4′-disulfonic acid (PPADS) and Brilliant Blue G (BBG) [7,8]. BBG is the prototypic antagonist, which blocks P2X$_7$R at a 10–100-times higher potency than any other receptor of the P2X family [9]. This receptor has been found in all cells of the immune system studied so far, and its prolonged activation results in extensive membrane blebbing over timescales ranging from seconds to minutes [1] and, eventually, in cell death [1,2]. The potent cytotoxicity that accompanies sustained stimulation of P2X$_7$R can be in part related to the ability of this receptor to drive the release of large amounts of IL-1ß, and other inflammatory cytokines from immune and inflammatory cells [10].

Upon transient stimulation, P2X$_7$R behaves like many other channels selective for mono- and divalent cations. However, the channel becomes nonselective upon sustained stimulation and begins to admit molecules with molecular weights up to 900 Da [5,11–14]. Virginio et al. [6] have suggested that the increase in permeability indicates that the permeation path undergoes a progressive dilation rather than a single-step transition from a small size to a large size. The long C-terminal domain is related to the dilation of this nonselective pore [3]. Pore dilatation was also observed in P2X$_2$R and in P2X$_4$R. However, in these channels, dilatation was reversible and it was not accompanied by a cytosolic effect. The opening velocity of these pores was estimated to be 1 Å s^{-1} [6].

Experimental studies suggested one trimeric arrangement for this receptor which can be arranged as homo or heterooligomers [15–20]. Recent X-ray crystallographic studies of P2X$_4$R indicated trimeric

* Corresponding author. Tel.: +55 21 2562 1815; fax: +55 21 2562 1816.
E-mail address: souzacam@ioc.fiocruz.br (L.A. Alves).

0005-2736/$ – see front matter © 2011 Elsevier B.V. All rights reserved.
doi:10.1016/j.bbamem.2011.09.010

functional organization [21]. When expressed heterologously, most P2X receptors (P2XR) isoforms form channels with distinct pharmacological and kinetic properties [15,22,23]. Their primary sequences contain between 379 ($P2X_1R$) and 595 ($P2X_7R$) amino acids, and a sequence alignment of the first 400 residues reveals more than 30% homology [9].

Topology prediction and hydrophobicity profiles indicate that each subunit of those receptors (P2X) comprises two transmembrane segments, TM1 and TM2, arranged such that the intracellular domain is formed by the amino and carboxy termini. The termini are separated by a large extracellular region containing 10 positionally conserved cysteine residues and a variable number of consensus sites for N-linked glycosylation [24,25]. Although the transmembrane topologies of P2XRs are similar to acid-sensing ion channels (ASICs, also known as ACCNs), epithelial sodium channels (ENaCs) and degenerin channels (DEGs) [21], inward-rectifier K^+ channels (Kir) [26], and mechanosensitive channels with large conductance (MscL) [27–29], there is little to no relationship between the primary amino acid sequences of P2XRs and these other channels. This topology is thus novel for ligand-gated channels [30]. Teixeira et al. demonstrated the possibility of a novel motif for the M2 domain of $P2X_7R$ called ADSEG. This peptide segment is a consensus segment located in the M2 domain that characterizes this motif [31].

Despite all of the findings described above, how the "large pore" forms is still unknown. We thus decided to perform an electrophysiological characterization of the consensus peptide (ADSEG) to shed light on the large pore formation mechanism of $P2X_7R$.

2. Materials and methods

2.1. Materials

2.1.1. Planar lipid membranes

E. coli polar lipid extract was purchased from Avanti Polar Lipids (Alabaster, AL, USA), and a 1.5% hexadecane–hexane mixture was obtained from Fluka (Berlin, Germany). The ADSEG sequence (FGIRFDILVFGTGGKFDIIQLVVY; amino acids 313–336) was synthesized by the Wittmann Institute of Technology and Analysis of Biomolecules (Berlin, Germany) at 95% purity, and the sequence was confirmed using a MALDI mass spectrum. Stock solutions of ADSEG peptide (4 μg/mL) were prepared using 2,2,2-trifluoroethanol (TFE) from Fluka (Berlin, Germany).The solutions contained (in mM) 2.5, 5, 10, 20, 80, 150 and 300 KCl, 2.5, 5, 10, 20, 80, 150 and 300 NaCl, 150 $MgCl_2$, 150 $CaCl_2$ from MERCK (Berlin, Germany). In some experiments 300 mM N-methyl-D-glucamine (NMDG, Fluka, Berlin, Germany) were used. All solutions were buffered with 10 mM HEPES, pH 7.4 (Fluka, Berlin, Germany).

2.1.2. Patch-clamp

Electrolyte solutions comprised of 150 mM KCl, 5 mM NaCl, 1 mM $MgCl_2$, 1 mM $CaCl_2$, 10 mM HEPES and 0.1 mM ethylene glycol tetraacetic acid (EGTA) (pH 7.4, 295 mOsm) were used in both pipette and bath. All chemicals were from Sigma (USA). In some experiments, the osmolarity of the solution was checked using a Welscor Model 5500 vapor pressure osmometer. RPMI 1640 medium was obtained from Sigma (USA) (pH 7.4) and 10% fetal calf serum from LGC (Brazil) and penicillin (100 U/mL) and streptomycin (100 μg/mL) from Sigma (USA) were added to the medium for cells grown.

2.2. Methods

2.2.1. Bioinformatics analyses

Sequence alignment analysis was performed using ClustalX (http://bips.u-strasbg.fr/fr/Documentation/ClustalX/) [32]. 3D image was generated by VMD 1.83 (Visual Molecular Dynamic) available from http://ks.uiuc.edu/Reaserch/vmd/ [33].

2.2.2. Bilayer preparation and activity measurements

Monolayers from 1.5% *E. coli* polar lipid extract solution in hexane were spread on top of two aqueous solutions (1.5 mL) separated by a Teflon diaphragm. After evaporation of hexane planar bilayers were formed by raising the water levels above the aperture (60 to 80 μm in diameter) in the diaphragm [34]. The diaphragm was pretreated with a solution consisting of 1% hexadecane dissolved in hexane. After membrane formation, the peptide was added from a TFE stock solution to one or both sides of the membrane to final concentrations of 1.4, 2.7 or 4.1 ng/mL. The buffer solutions were agitated by magnetic stirring bars. The final concentration of TFE did not exceed 0.5%, and control experiments with TFE showed that this solvent did not alter membrane conductance. Bilayer formation and thinning were monitored by capacitance measurements and optical observation. Electrical measurements were conducted under voltage clamp conditions using Ag/AgCl electrodes and agar salt bridges (500 mM KCl) which were immersed in the buffer solutions on both sides of the membrane. The measurements were performed using a current amplifier (model VA-10, NPI, Tamm, Germany) connected to an analog–digital interface from National Instruments. Using WinEDR (Strathclyde Electrophysiology Software) we recorded the current in intervals of 320 s and filtered them at 13.00 Hz. The raw data were analyzed using ORIGIN 7.0 and/or Sigma Plot (Microcal Software). We applied voltages of −30 mV, 30 mV, −60 mV, 60 mV, −90 mV and 90 mV to the trans side of the membrane.

2.2.3. Cell preparations and patch-clamp recordings

Human embryonic kidney (HEK 293) cells were kindly provided by the cell bank of the Clementino Fraga University Hospital (Rio de Janeiro, Brazil). These cells were cultured in RPMI 1640 medium containing fetal calf serum (10%), penicillin (100 u/mL) and streptomycin (100 μg/mL) and then plated onto 35 mm Petri dishes for 2–5 days before use.

To monitor the single channel ADSEG current, the gigaOhm seal patch-clamp technique was applied in cell-attached configuration. Patch clamping was performed at 37 °C using an Axopatch-1D amplifier (Axon Instruments, San Mateo, USA). HEK 293 cells were transferred to a chamber mounted on a microscope stage. A high-resistance seal (1–10 GΩ) was established by gentle suction, the cell membrane beneath the tip of the electrode was disrupted by additional suction. The recordings were accepted if the current and membrane conductance returned to within 1–5% of the control values after agonist application, which indicates that the large increase in conductance was not due to cell lysis with loss of the seal. The series resistance ranged from 6 to 10 MΩ in all experiments, and no compensation was applied to currents <400 pA. Currents above this level were compensated by 85%. Experiments in which the series resistance increased substantially during the measurement were discarded. The cell capacitance was measured by applying a 20 mV hyperpolarizing pulse from a holding potential of −60 mV, and the capacitive transient was integrated and divided by the amplitude of the voltage step (20 mV). The measured currents were filtered with a corner frequency of 5 kHz (8-pole Bessel filter), digitized at 20–50 kHz using a Digidata 1320 interface (Axon Instruments, Palo Alto, CA, USA) and acquired on a personal computer using the pClamp 9.0 software.

The pipette was filled with the solution as previously described. The pipette was then inserted over a period of 10 s into an Eppendorf tube containing the peptide, which was diluted (100 ng) to allow it to enter the pipette by capillary action.

2.3. Determination of single channel open probability

Although recordings containing only a single opening channel are ideal for performing a kinetic analysis, many recordings contain multiple opening channels and must be analyzed using a

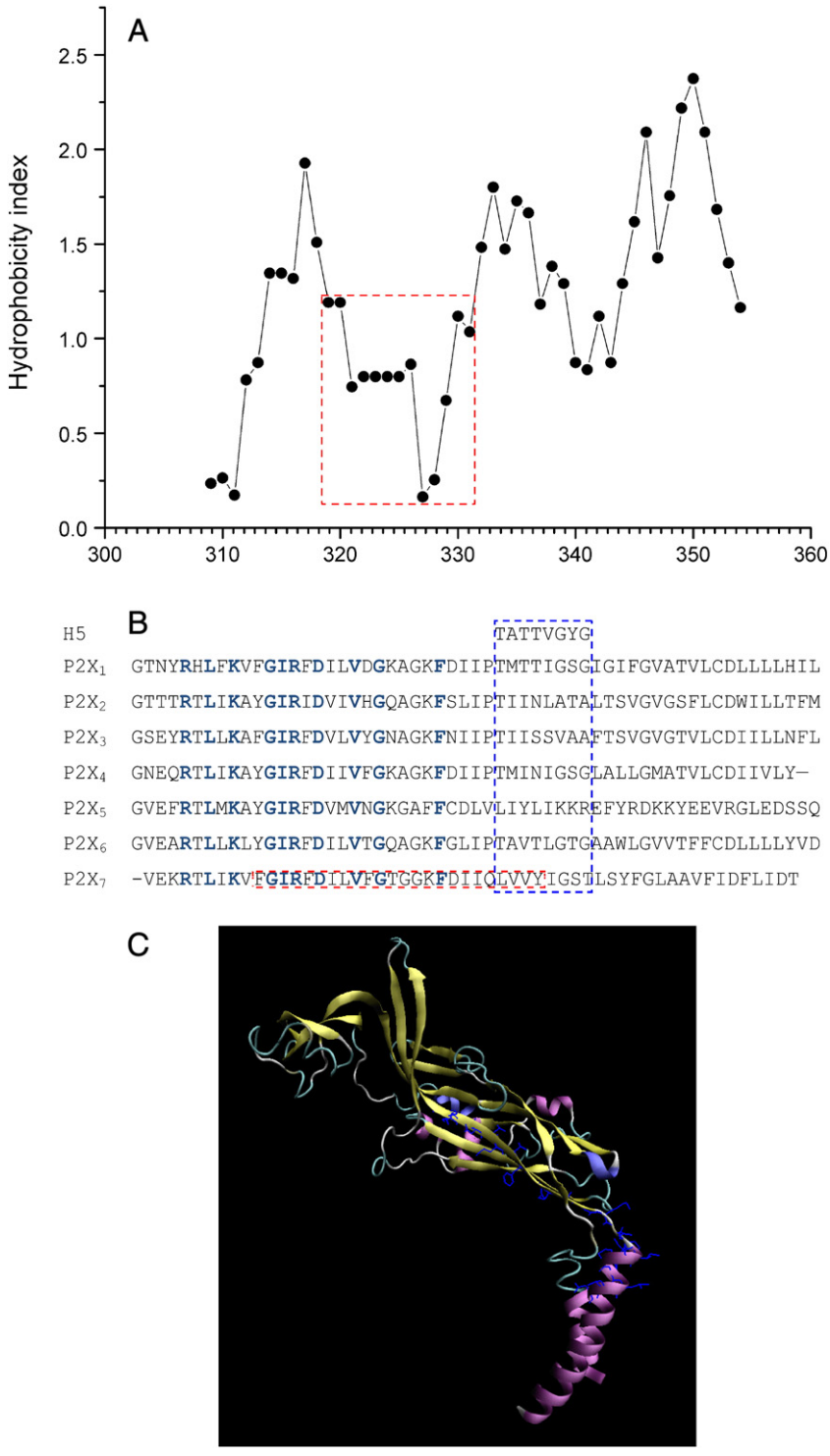

Fig. 1. Analyses of ADSEG primary sequence. (A) Hydrophobicity graph of the M2 domain of hP2X$_7$R. Hydrophobicity values were calculated according to the Kyte and Doolittle scale and are plotted against the amino acid sequence (window 21). The red box represents the ADSEG (313–336 residues) in M2 domain. (B) ClustalX Multiple alignments among all M2 sequences of P2XR subtypes and H5 signature segment of K^+ channel; blue residues indicate highly conserved M2 residues. The red box shows the residues that compose the ADSEG sequence and the blue box shows the residues that pair with the H5 signature segment. (C) 3D image of the ADSEG segment putative location in the P2X$_4$R represented as blue residues by VMD program.

previously reported method [35]. The activity of a single-channel is given by:

$$NP_0 = \sum_{i=0}^{N_A} \frac{it_i}{T}$$

where N is the total number of functional channels, determined by observing the number of peaks detected in all-points amplitude histograms, T is the total recording time, N_A is the apparent number of channels in the recordings, determined from the highest observed current level, i is the number of open channels and t_i is the time during which the i channels are open.

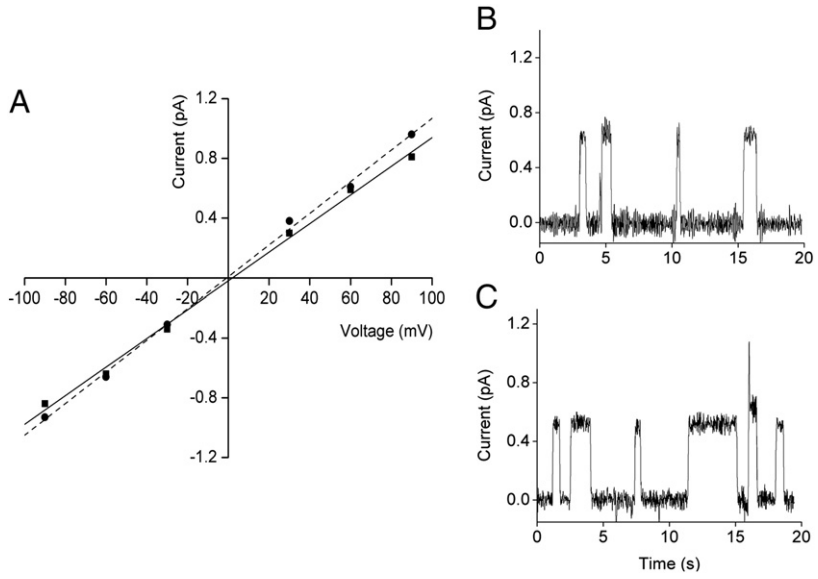

Fig. 2. Currents of ADSEG in planar lipid bilayer. (A) Current × voltage relation of ADSEG added only in one side (■) and in both sides (●); increasing range of voltage was applied (from −90 mV to +90 mV; voltage step of 30 mV). (B) Records of single channels of 1.4 ng/mL ADSEG at 2.5 mM KCl and 10 mM HEPES (pH 7.4) added in trans side and (C) in both side at holding potential of +60 mV. Lines are the best-fit linear least squares regression line through the data points. Representative results from at least three experiments are shown.

If the single-channel recordings contain no overlapping opening events, then t_0 can be determined unambiguously, and the open probability P_0 of a single-channel can be calculated from:

$$P_0 = \frac{t_0}{t_0 + t_{\text{closed}}}$$

where P_0 is the probability that the channel is open, t_0 is the average amount of time that the channel is open and t_{closed} is the average amount of time that the channel is closed [35]. WINEDR 3.0.6 (Strathclyde Electrophysiology Software) was used to analyze the data, obtain the parameters required to calculate the open probability from the data measured in the lipid bilayer and patch-clamp experiments.

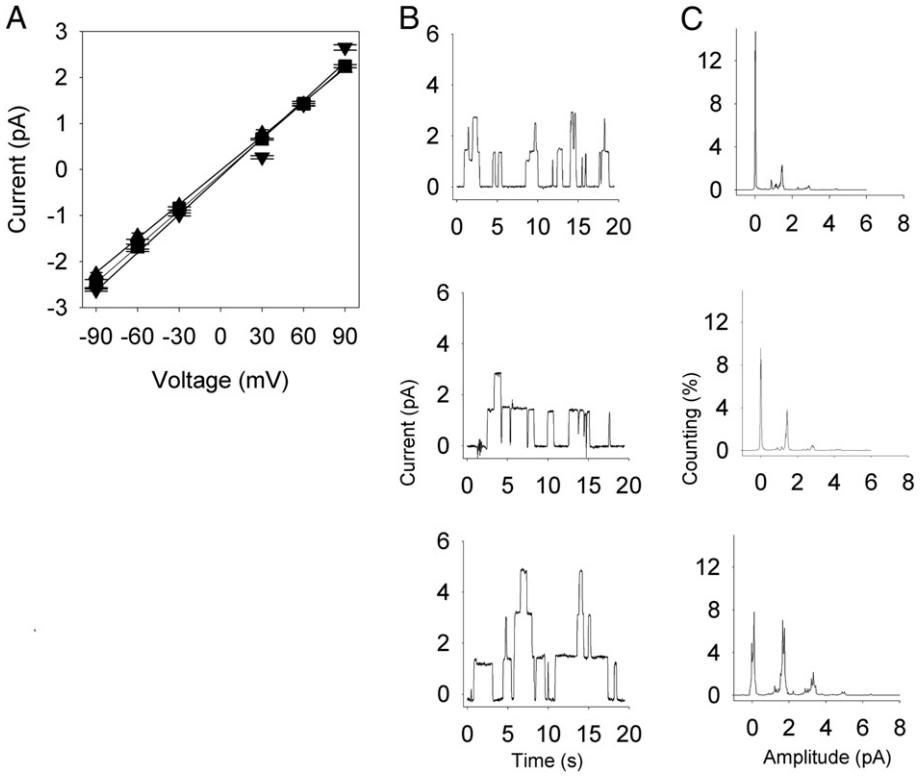

Fig. 3. Single channel activity dependent of ADSEG concentration. (A) Current–voltage relation of ADSEG. For recordings conditions bath contained 150 mM KCl and 10 mM HEPES (pH 7.4) in both sides and an increasing range of voltage was applied (from −90 mV to +90 mV; voltage step of 30 mV); different concentrations of ADSEG were added in both sides: (■) 1.4, (▲) 2.7 and (▼) 4.1 ng/mL. (B) Graphics and the respective histograms (C) of the current records for the different ADSEG concentrations at holding potential at +60 mV. Lines are the best-fit linear least squares regression line through the data points. Representative results from at least three experiments are shown.

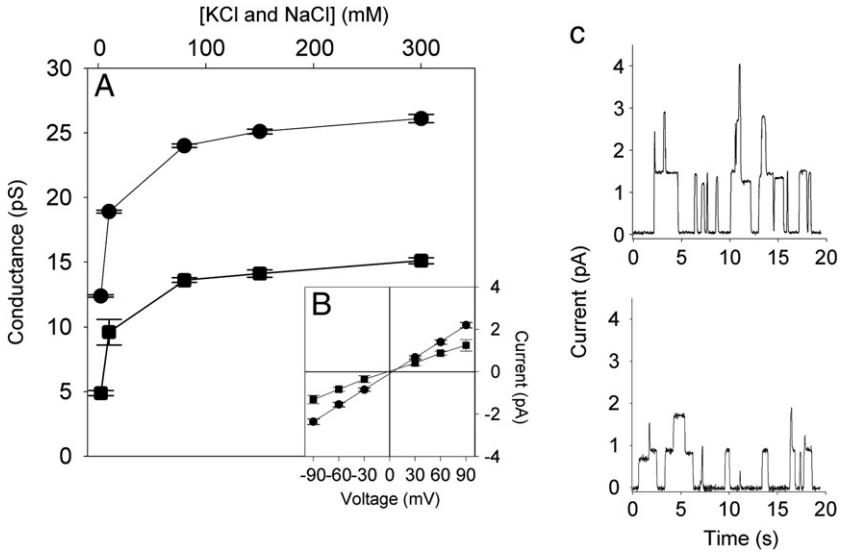

Fig. 4. Single channel conductances of different monovalent ions. The conductances of K^+ and Na^+ were measured by adding 1.4 ng/mL ADSEG and increasing concentrations of K^+ or Na^+ to both compartments. (A) Conductances were plotted against the increasing (●) KCl and (■) NaCl concentrations (2.5, 10, 80, 150 and 300 mM). (B) Current–voltage relation at (●) 150 mM KCl and (■) 150 mM NaCl increasing range of voltage was applied (from −90 mV to +90 mV; voltage step of 30 mV). (C) Representative single channel recordings of 150 mM K^+ and 150 mM Na^+ respectively at holding potential of +60 mV. Lines are the best-fit linear least squares regression line through the data points. Representative results from at least three experiments are shown.

2.4. Statistical analysis

Data are expressed as mean values of at least three independent experiments ±SE (standard error). Linear regression and Pearson correlation coefficient were determinate by the correlation function CORREL in Microsoft Exel program.

3. Results

3.1. Channel formation in artificial planar lipid bilayers

ADSEG is formed by a large portion of the consensus sequence of the hydrophobic M2 domain (Fig. 1A) and includes some of the residues that align with the H5 signature segment (Fig. 1B).The peptide was selected based on ClustalX multiple sequence alignments (Fig. 1B) which revealed residues with 100% identity among all $P2X_7$ subtypes (red dashed line). To illustrate the putative ADSEG location, its residues are highlighted in blue in the $P2X_4R$ 3D image (Fig. 1C).

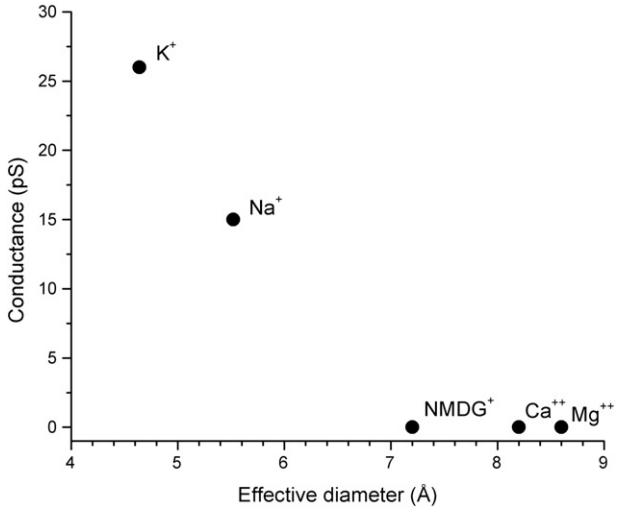

Fig. 5. Conductance of single ADSEG channels for each cation tested. Different mono and divalent ions (in 150 mM K^+, Na^+, Ca^{2+}, Mg^{2+} and 300 mM $NMDG^+$) were applied to the planar lipid bilayer in both sides of the chamber in the presence of 1.4 ng/mL ADSEG. Conductance profile was evaluated by the effective diameter of each cation in Å. Representative results from at least three experiments are shown.

We first addressed the question whether the ADSEG peptide inserts into artificial lipid membranes and forms channels. Therefore, we added ADSEG to both sides (cis and trans) or to only one side (trans) of the membrane (final concentration 1.4 ng/mL) from an ethanolic stock solution. ADSEG insertion resulted in channel activity, which was similar to unilateral (Fig. 2B) or bilateral (Fig. 2C) additions. Single channel conductance did not depend on voltage (Figs. 2A, 3A). The total membrane current increased with increasing dose (Fig. 3). ADSEG activity did not change in an interval of 2 h indicating that ADSEG is stable in solution.

To investigate a possible relationship between the open probability of the channels and the concentration of ADSEG, we plotted the channel open probabilities in lipid bilayers and biological membranes against different peptide concentrations (Fig. S1A, B). Both graphs show that the Pearson correlation index between the probability of open channels and the peptide concentration is very small, taking the values 0.35 and −0.50 for planar lipid bilayers (Fig. S1A) and membrane patches (Fig. S1B), respectively. Therefore, we consider the channel open probabilities (0.22 for planar lipid bilayers and 0.24 for biological membranes) to be independent of peptide concentration. It is also interesting that channels formed at much lower ADSEG concentrations in planar lipid bilayers, suggesting that the crowded environment of biological membranes somehow decreases reconstitution efficiency.

3.2. Salt concentration dependence

We evaluated the dependence of ADSEG single channel conductance on salt concentration by adding 1.4 ng peptide/mL to both sides of the chamber and by varying the KCl and NaCl concentrations between 2.5 and 300 mM (Fig. 4A). The K^+ conductance exceeds the Na^+ conductance (Fig. 4B inset). Saturation occurred for both KCl and NaCl at a concentration of 80 mM (Fig. 4A). Fig. 4C displays representative single channel recordings of 150 mM K^+ and 150 mM Na^+ respectively at holding potential of +60 mM.

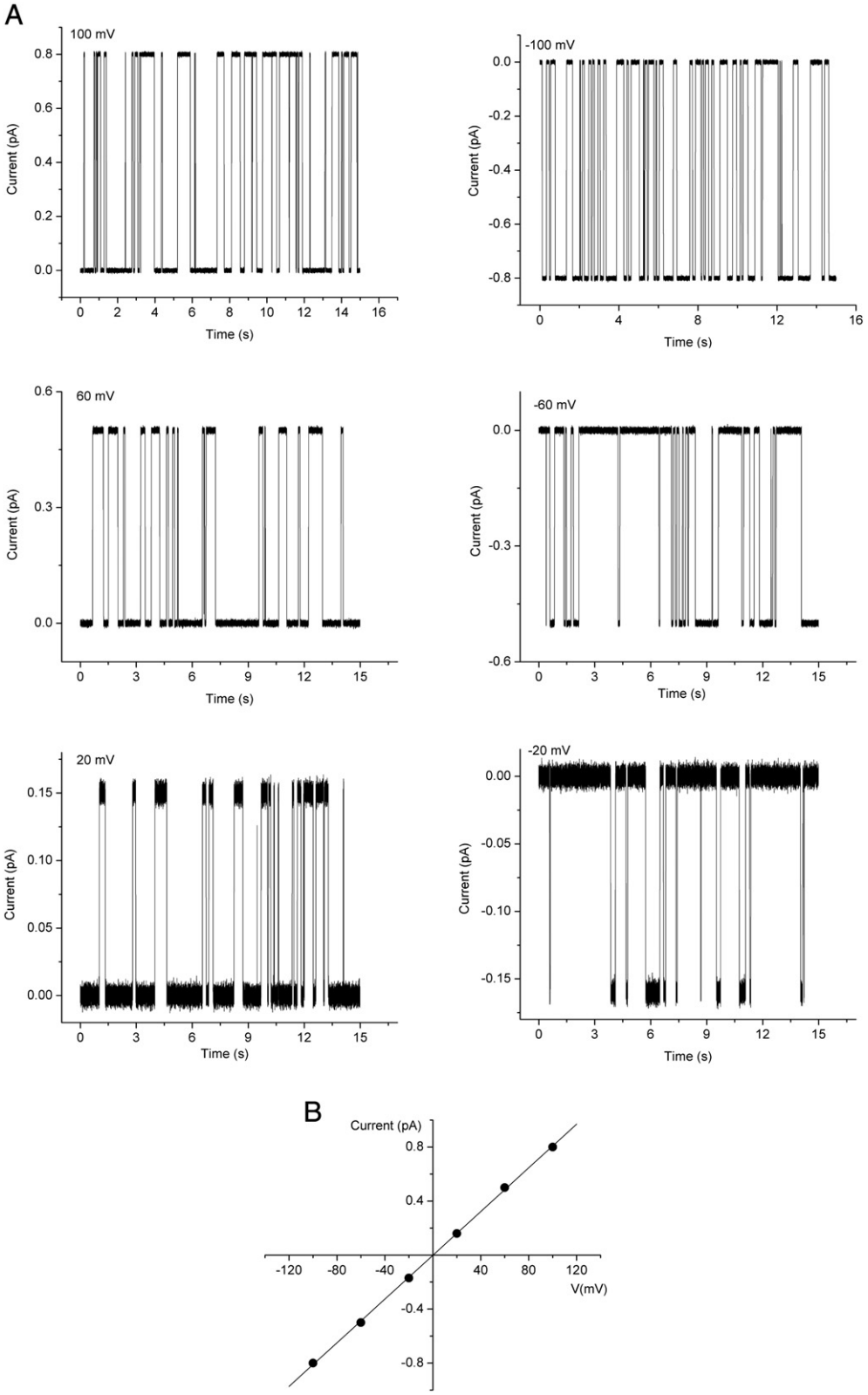

Fig. 6. Single channel conductance in patch-clamp. (A) ATP-gated currents after 250 ng/mL ADSEG addition in 150 mM KCl, pH 7.4 from HEK 293 cells at increasing range of voltage (from −100 mV to 100 mV). Holding potential of −40 mV. (B) Mean current–voltage relation of the ADSEG for the cell-attached recording. Representative results from at least three experiments performed on different days.

3.3. Determination of the effective channel diameter of the ADSEG channel

The unitary conductance of ion channels generally depends on crystal radius or hydration radius of the ions (effective radius). In the absence of interacting residues in the channel, which may act as a surrogate for the water of hydration, channel selectivity is expected to mirror the differences in mobility of the hydrated ions. The selectivity of ADSEG channels is in line with these considerations as

revealed by the plot of channel conductance against the effective diameter of K^+, Na^+, Mg^{2+}, Ca^{2+} [36] and NMDG [37] (4.64 Å, 5.52 Å, 8.6 Å, 8.2 Å, and 7.2 Å respectively) (Fig. 5). The channels are impermeable to divalent and monovalent cations with an effective diameter equal or greater than 7.2 Å.

3.4. Channel activity in mammalian cell membranes

We performed patch-clamp experiments in the cell-attached configuration using HEK 293 cells. Fig. 6A displays representative recordings of ADSEG channels at different holding potentials. Fig. 6B illustrates the single channel current–voltage relationship of channels formed after peptide reconstitution. A linear regression analysis yielded a slope (conductance) of 8.08 ± 0.08 pS when 150 mM KCl was present in the pipette. In the absence of ADSEG, neither pore formation nor low-amplitude channel conductance was observed (data not shown).

4. Discussion

We have studied the functionality of the ADSEG consensus peptide from the TM2 segment of P2X receptors [31]. This segment is thought to be involved in the formation of a cation-selective pore and in the formation of a non-selective pore associated with $P2X_7R$. Using artificial bilayers and biological membranes, we demonstrated channel activity. Its characteristics are similar to those of the full-length channel: K^+ conductance is equal to 8.08 ± 0.08 pS under patch-clamp conditions and to 8.0 ± 0.3 pS for $P2X_7R$ [38]. The open probabilities (K^+) of the channels are equal to 0.22 and 0.24 in lipid bilayers and in membrane patches, which is comparable to the full-length $P2X_7R$ (0.26) [1].

The conductances of channels in lipid bilayers depend on the effective diameter of the conducted cations. ADSEG conductivity for K^+ was larger than that for Na^+. This result is in contrast to the pattern found for $P2X_7R$ [37]. The conductance for Na^+ is higher than that for K^+, differing of the expected to aqueous solution where the hydration radius and the conductance are inversely proportional, indicating the presence of a selectivity filter in this receptor [39]. ADSEG also failed to conduct cations with an effective diameter greater than 7.2 Å. This size limit is in agreement with the value of 8 Å found by Virginio et al. [6] for the nondilated pore of rat $P2X_7R$ expressed in HEK 293 cells.

Several properties of ion channels have been analyzed in artificial lipid bilayers. In most studies, the distinctions between cations and anions are well-preserved in bilayer systems when using synthetic peptides that have sequences equal to the transmembrane segments putatively responsible for pore formation [13,40,41]. Synthetic peptides corresponding to the M2 segment of glycine receptors and to the M2 and M6 segments of the cystic fibrosis chloride channel formed anionic channels [40,42], while the synthetic peptide from the M2 nicotinic cholinergic receptor formed a cationic channel. In this study, the cationic nature of $P2X_7R$ was preserved as expected in the segment participating in channel formation. The consensus segment has a net negative charge that is likely due to two aspartate residues in the sequence that are balanced by only one positive charge.

It should be emphasized that the activation of the $P2X_7R$ gives rise to a low-conductance channel (<15 pS) and an associated pore (>300 pS) that allows the passage of dyes with molecular weight of at least 1 kDa. Thus, it is important to point out that our data do not reveal any high-conductance channel compatible with the model of a pore associated with $P2X_7R$, which reinforces the idea that other proteins associated with $P2X_7R$ form the pore that is permeable to dyes larger than 1 kDa. One can argue that a small peptide would not form a pore consistent with conductance levels beyond 300 pS. However, studies have shown that peptides with 10 and 24 residues, respectively, can form high-conductance channels [43,44] e.g. by spontaneous oligomerization and self-assembly into larger structures. It is well possible that ADSEG channel activity generally requires oligomerization. However, our experiments did not allow testing that possibility. We have also tested the entire sequence of recombinant $P2X_7$ protein in our system (data not shown) but did not observe any channel formation. We cannot explain this at present, although it is known that some integral proteins do not reconstitute in artificial bilayers [45].

For the first time, we have demonstrated that a conserved and hydrophobic part of the M2 segment can form ion channels in lipid bilayers. They have properties similar to those of the full $P2X_7$ channel. Further efforts are required to clarify which residues participate to the pore opening and how dilatation of the pore non-selective occurs.

Supplementary materials related to this article can be found online at doi:10.1016/j.bbamem.2011.09.010.

Acknowledgments

This work was supported from the Fundação Oswaldo Cruz (FIOCRUZ — Rio de Janeiro, Brazil), Fundação de Amparo à Pesquisa do Estado do Rio de Janeiro, Brazil and the Forschunginstitut Molekular Pharmakologie (Berlin, Germany). We are grateful to Dr. Sergio Noboru Kuriyama and Roberta G. Bortolini for their helpful discussions and to Dr. Sapar Saparov† (in memorium) and Matthias Prige for helping us with certain experiments.

References

[1] C. Virginio, A. MacKenzie, R.A. North, A. Surprenant, Kinetics of cell lysis, dye uptake and permeability changes in cells expressing the rat P2X7 receptor, J. Physiol. 519 (Pt 2) (1999) 335.
[2] G.R. Dubyak, Purinergic signaling at immunological synapses, J. Auton. Nerv. Syst. 81 (2000) 64.
[3] F. Rassendren, G. Buell, A. Newbolt, R.A. North, A. Surprenant, Identification of amino acid residues contributing to the pore of a P2X receptor, EMBO J. 16 (1997) 3446.
[4] C. Kennedy, G. Burnstock, Evidence for two types of P2-purinoceptor in longitudinal muscle of the rabbit portal vein, Eur. J. Pharmacol. 111 (1985) 49.
[5] R.A. North, Molecular physiology of P2X receptors, Physiol. Rev. 82 (2002) 1013.
[6] C. Virginio, A. MacKenzie, F.A. Rassendren, R.A. North, A. Surprenant, Pore dilation of neuronal P2X receptor channels, Nat. Neurosci. 2 (1999) 315.
[7] B. Sperlagh, E.S. Vizi, K. Wirkner, P. Illes, P2X7 receptors in the nervous system, Prog. Neurobiol. 78 (2006) 327.
[8] C.M. Anderson, M. Nedergaard, Emerging challenges of assigning P2X7 receptor function and immunoreactivity in neurons, Trends Neurosci. 29 (2006) 257.
[9] B.S. Khakh, G. Burnstock, C. Kennedy, B.F. King, R.A. North, P. Seguela, M. Voigt, P.P. Humphrey, International union of pharmacology. XXIV. Current status of the nomenclature and properties of P2X receptors and their subunits, Pharmacol. Rev. 53 (2001) 107.
[10] P.G. Baraldi, M.C. Nunez, M. Morelli, S. Falzoni, Synthesis and Biological Activity of N-Arylpiperazine Modified Analogues of KN-62, a Potent Antagonist of the Purinergic P2X7 Receptor, J. Med. Chem. 46 (2003) 1318.
[11] F. Di Virgilio, S. Falzoni, P. Chiozzi, J.M. Sanz, D. Ferrari, G.N. Buell, ATP receptors and giant cell formation, J. Leukoc. Biol. 66 (1999) 723.
[12] K.T. Le, K. Babinski, P. Seguela, Central P2X4 and P2X6 channel subunits coassemble into a novel heteromeric ATP receptor, J. Neurosci. 18 (1998) 7152.
[13] R.A. North, E.A. Barnard, Nucleotide receptors, Curr. Opin. Neurobiol. 7 (1997) 346.
[14] G.E. Torres, W.R. Haines, T.M. Egan, M.M. Voigt, Co-expression of P2X1 and P2X5 receptor subunits reveals a novel ATP-gated ion channel, Mol. Pharmacol. 54 (1998) 989.
[15] A. Nicke, H.G. Baumert, J. Rettinger, A. Eichele, G. Lambrecht, E. Mutschler, G. Schmalzing, P2X1 and P2X3 receptors form stable trimers: a novel structural motif of ligand-gated ion channels, EMBO J. 17 (1998) 3016.
[16] L.H. Jiang, M. Kim, V. Spelta, X. Bo, A. Surprenant, R.A. North, Subunit arrangement in P2X receptors, J. Neurosci. 23 (2003) 8903.
[17] A. Aschrafi, S. Sadtler, C. Niculescu, J. Rettinger, G. Schmalzing, Trimeric architecture of homomeric P2X2 and heteromeric P2X1+2 receptor subtypes, J. Mol. Biol. 342 (2004) 333.
[18] N.P. Barrera, S.J. Ormond, R.M. Henderson, R.D. Murrell-Lagnado, J.M. Edwardson, Atomic force microscopy imaging demonstrates that P2X2 receptors are trimers but that P2X6 receptor subunits do not oligomerize, J. Biol. Chem. 280 (2005) 10759.
[19] K. Mio, Y. Kubo, T. Ogura, T. Yamamoto, C. Sato, Visualization of the trimeric P2X2 receptor with a crown-capped extracellular domain, Biochem. Biophys. Res. Commun. 337 (2005) 998.

[20] G.R. Dubyak, Go it alone no more — P2X7 joins the society of heteromeric ATP-gated receptor channels, Mol. Pharmacol. 72 (2007) 1402.
[21] T. Kawate, J.C. Michel, W.T. Birdsong, E. Gouaux, Crystal structure of the ATP-gated P2X(4) ion channel in the closed state, Nature 460 (2009) 592.
[22] R. Stoop, S. Thomas, F. Rassendren, E. Kawashima, G. Buell, A. Surprenant, R.A. North, Contribution of individual subunits to the multimeric P2X(2) receptor: estimates based on methanethiosulfonate block at T336C, Mol. Pharmacol. 56 (1999) 973.
[23] M. Kim, O.J. Yoo, S. Choe, Molecular assembly of the extracellular domain of P2X2, an ATP-gated ion channel, Biochem. Biophys. Res. Commun. 240 (1997) 618.
[24] A.J. Brake, M.J. Wagenbach, D. Julius, New structural motif for ligand-gated ion channels defined by an ionotropic ATP receptor, Nature 371 (1994) 519.
[25] S. Valera, N. Hussy, R.J. Evans, N. Adami, R.A. North, A. Surprenant, G. Buell, A new class of ligand-gated ion channel defined by P2X receptor for extracellular ATP, Nature 371 (1994) 516.
[26] R.A. Schwalbe, C.S. Wingo, S.L. Xia, Mutations in the putative pore-forming segment favor short-lived wild-type Kir2.1 pore conformations, Biochemistry 41 (2002) 12457.
[27] P.C. Moe, P. Blount, C. Kung, Functional and structural conservation in the mechanosensitive channel MscL implicates elements crucial for mechanosensation, Mol. Microbiol. 28 (1998) 583.
[28] S.I. Sukharev, P. Blount, B. Martinac, F.R. Blattner, C. Kung, A large-conductance mechanosensitive channel in *E. coli* encoded by mscL alone, Nature 368 (1994) 265.
[29] S.I. Sukharev, P. Blount, B. Martinac, C. Kung, Mechanosensitive channels of *Escherichia coli*: the MscL gene, protein, and activities, Annu. Rev. Physiol. 59 (1997) 633.
[30] M.O. Ortells, G.G. Lunt, Evolutionary history of the ligand-gated ion-channel superfamily of receptors, Trends Neurosci. 18 (1995) 121.
[31] P.C. Teixeira, C.A. de Souza, M.S. de Freitas, D. Foguel, E.R. Caffarena, L.A. Alves, Predictions suggesting a participation of beta-sheet configuration in the M2 domain of the P2X(7) receptor: a novel conformation? Biophys. J. 96 (2009) 951.
[32] J.D. Thompson, T.J. Gibson, F. Plewniak, F. Jeanmougin, D.G. Higgins, The ClustalX windows interface: flexible strategies for multiple sequence alignment aided by quality anlysis tools, Nucleic Acids Res. 24 (1997) 4876.
[33] W. Humphrey, A. Dalke, K. Schulten, VMD: visual molecular dynamics, J. Mol. Graph. 14 (1996) 33.
[34] S.T. White, The physical nature of planar bilayer membrane, in: C. Miller (Ed.), Ion Channel Reconstitution, Plenum, New York, 1986, pp. 3–35.
[35] G. Yue, D. Merlin, M.E. Selsted, W.I. Lencer, J.L. Madara, D.C. Eaton, Cryptdin 3 forms anion selective channels in cytoplasmic membranes of human embryonic kidney cells, Am. J. Physiol. Gastrointest. Liver Physiol. 282 (2002) G757–G765.
[36] B. Tansel, J. Sager, T. Rector, J. Garland, R.F. Strayer, L. Levine, M. Roberts, M. Hummerick, J. Bauer, Significance of hydrated radius and hydration shells on ionic permeability during nanofiltration in dead end and cross flow modes, Sep. Purif. Technol. 51 (2006) 40.
[37] T. Riedel, G. Schmalzing, F. Markwardt, Influence of extracellular monovalent cations on pore and gating properties of P2X7 receptor-operated single-channel currents, Biophys. J. 93 (2007) 846.
[38] T. Riedel, I. Lozinsky, G. Schmalzing, F. Markwardt, Kinetics of P2X7 receptor-operated single channel currents, Biophys. J. 92 (2007) 2377.
[39] K. Migita, R.H. Willlian, M.M. Voigt, M.E. Terrances, Polar Residues of the Second Transmembrane Domain Influence Cation Permeability of the ATP-Gated P2X2 Receptor, J. Biol. Chem. 276 (2001) 30934.
[40] D. Langosch, K. Hartung, E. Grell, E. Bamberg, H. Betz, Ion channel formation by synthetic transmembrane segments of the inhibitory glycine receptor — a model study, Biochim. Biophys. Acta 1063 (1991) 36.
[41] M. Oblatt-Montal, L.K. Buhler, T. Iwamoto, J.M. Tomich, M. Montal, Synthetic peptides and four-helix bundle proteins as model systems for the pore-forming structure of channel proteins. I. Transmembrane segment M2 of the nicotinic cholinergic receptor channel is a key pore-lining structure, J. Biol. Chem. 268 (1993) 14601.
[42] G.L. Reddy, T. Iwamoto, J.M. Tomich, M. Montal, Synthetic peptides and four-helix bundle proteins as model systems for the pore-forming structure of channel proteins. II. Transmembrane segment M2 of the brain glycine receptor is a plausible candidate for the pore-lining structure, J. Biol. Chem. 268 (1993) 14608.
[43] J. Thundimadathil, R.W. Roeske, L. Guo, A synthetic peptide forms voltage-gated porin-like ion channels in lipid bilayer membranes, Biochem. Biophys. Res. Commun. 330 (2005) 585.
[44] Y.N. Antonenko, T.B. Stoilova, S.I. Kovalchuk, N.S. Egorova, A.A. Pashkovskaya, A.A. Sobko, E.A. Kotova, S.V. Sychev, A.Y. Surovoy, Large unselective pore in lipid bilayer membrane formed by positively charged peptides containing a sequence of gramicidin A, FEBS Lett. 579 (2005) 5247.
[45] Christopher Miller, Ion Channel Reconstitution, Plenum Press, New York, 1986.